Singapore Management University

Institutional Knowledge at Singapore Management University

Research Collection School Of Information Systems

School of Information Systems

8-2014

A palm vein identification system based on Gabor wavelet features

Ran WANG

Guoyou WANG

Zhong CHEN

Zhigang ZENG

Yong WANG
Singapore Management University, yongwang@smu.edu.sg

Follow this and additional works at: https://ink.library.smu.edu.sg/sis_research

Part of the Programming Languages and Compilers Commons, and the Software Engineering Commons

Citation

1

ICONIP 2012

A palm vein identification system based on Gabor wavelet features

**Ran Wang · Guoyou Wang · Zhong Chen ·
Zhigang Zeng · Yong Wang**

Abstract As a new and promising biometric feature, thermal palm vein pattern has drawn lots of attention in research and application areas. Many algorithms have been proposed for authentication since palm vein has special characteristics, such as liveness detection and hard to forgery. However, the detection accuracy of palm vein quite depends on the preprocessing and feature representation, which is supposed to be translation and rotation invariant to some extent. In this paper, we proposed an effective method for palm vein identification based on Gabor wavelet features which contains five steps: image acquisition, ROI detection, image preprocessing, features extraction, and matching. The 178 palm vein images from 101 persons were used to test the proposed palm vein recognition approach, where 176 images were correctly recognized with two in failure. The experimental results demonstrate the effectiveness of the proposed approach.

Keywords Palm vein · Biological identification · Gabor wavelet

1 Introduction

Biological identification is one of the most important research issues in bioinformatics, which have been widely used in various fields [1, 2, 7, 21]; especially, in recent years, the personal identification using vein patterns has been impressive because of its value of application in

R. Wang · G. Wang · Z. Chen (✉) · Z. Zeng · Y. Wang
School of Automation, Huazhong University of Science and Technology, 1037 Luoyu Road, Hongshan District, Wuhan 430074, Hubei Province, People's Republic of China
e-mail: henpacked@163.com

security systems. The following five collected properties are able to prove it to be a promising research focusing in the biometric identification field: (1) all the biometric characteristics embodied by the vein patterns are typically universal and unique [2]; (2) veins underneath the surface of the palm are relatively stable with the growth of age [3]; (3) vein pattern is hard for intruders to forge or change due to its inside characteristic, and it is superior to the traditional fingerprint methods that would be fail if the fingerprints are ruined [4]; (4) objects who are going to be checked must be alive in the condition that thermal infrared can work [5]; (5) the process is more comfortable and friendly compared with DNA and iris pattern recognition [6].

The typical methods for palm vein pattern identification were proposed in [8, 9]. These methods first extract the feature points of vein pattern (junctions and endings) from the ROI of the original input image. And then implement the multiple resolution analysis (MRA) on FPVPs. Finally, the feature-match of the vein pattern images is accomplished for the identification. The above papers demonstrate the methods' effect by using the experiments. However, these methods' accuracy rate would be affected by the loss of a number of minutiae, as well as drops with the increasing subjects because the feature points are not enough to describe the shape of the palm vein pattern.

An improved method in [4] is simple and easy for hardware algorithm design. It includes five individual processing stages: hand image acquisition, image enhancement, vein pattern segmentation, skeletonization and matching. The 108 blood vessels images have been verified correctly and accurately using this method. Similarly in the method in [10], the similarity of two palm images is calculated by template matching. However, although the attractive verification rates have been stated, it

is not illustrated in the above papers whether skeleton or binary of palm vein image is enough for identification based on image matching.

To address the problems mentioned above, the appearance-based methods, such as eigenvein and Laplacianpalm features [11, 12], were proposed to represent palm veins. In [11], an alternate two-dimensional PCA was presented to exploit the correlation of vein features between images. In [12], a palm representation called Laplacianpalm was proposed that finds local information and yields a palm space to best detect the essential manifold structure. Therefore, these methods cannot effectively exploit both global and local features of palm veins, which play an important role in recognition [13].

According to the above analysis, a palm vein identification system based on Gabor wavelet transform is proposed in this paper. Although some well-known techniques and algorithms are introduced into our method, many innovative processes different from existing methods are presented. The main contributions of this paper are as below.

Because the palm veins in the image are not very clear suffering from messy palm prints, it is difficult to extract features of vein patterns. For such input pictures with poor quality, we design a sequence of preprocessing steps that enhances the contrast between palm vein patterns and background using contrast limited adaptive histogram equalization (CLAHE), alleviates negative influences by palm prints using a 2-D Gaussian low-pass filter, and removes isolated noise around the vein patterns using morphological methods.

Different from the existing popular methods, there are two reasons that we adopt Gabor wavelet features as the representation of palm vein patterns in the skeleton image. One reason is that the Gabor-based method [14] can effectively analyze variations in the intensity which reflect most of the random shape information in the skeleton image of palm veins. The other reason is that Gabor wavelet features are not sensitive to rotation and shift variations, which are quite common and inevitable on the stage of data acquisition.

The rest of this paper is organized as follows. Section 2 illustrates the proposed methods step by step in detail. Section 3 provides experimental results and discussions. And some important conclusions are given in Sect. 4.

2 Methods

The proposed palm vein verification method is shown in Fig. 1, which includes five steps: image acquisition, enhancement, segmentation, skeletonization and matching. Detailed descriptions of these five steps are introduced in the following sections.
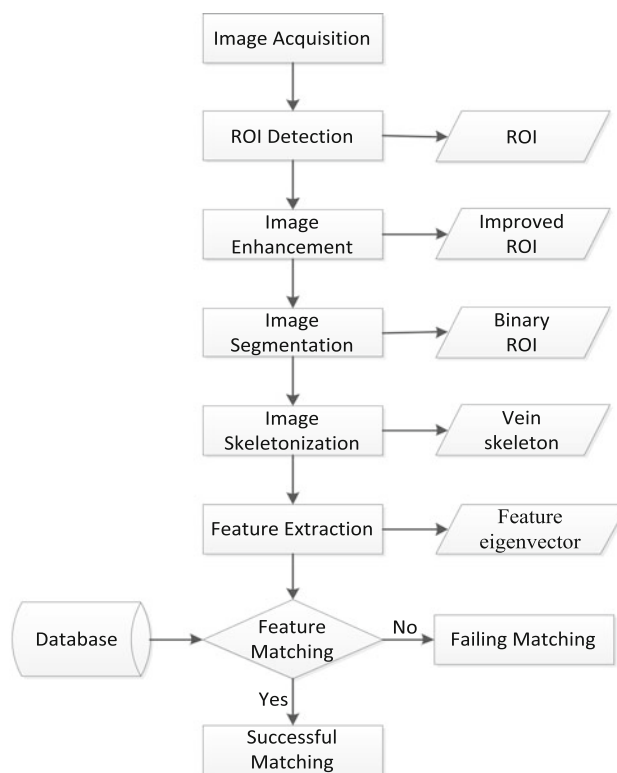

Fig. 1 Process of palm vein identification

2.1 Image acquisition

As there is no publicly available palm vein pattern database for research purpose, we establish our own near-infrared (NIR) palm vein pattern image database. A NIR charge-coupled device (CCD) camera is adopted as an input device for capturing palm vein images. Although principally being designed for use in visible light, these CCD cameras are also sensitive to NIR wavelengths of the electromagnetic spectrum up to nearly 1,100 nm. This is within the actinic IR range, which covers the NIR spectrum from 700 to 1,400 nm [13]. Besides, it has the benefits of high availability, good image quality and low cost. In our work, the NIR light source (LEDs) is evenly and circularly located around the camera and peaks at 850 nm wavelength. It should also be noted that an optical infrared filter is supposed to be mounted in front of the camera's lens since the CCD is also sensitive to visible light. And to achieve the best acquisition, the user should put his/her hand on a plane in front of the camera with the fingers spreading naturally at a fixed distance about 25 cm away from the cameras. Then, palm vein images can be obtained from the CCD sensor with NIR light source. In order to achieve accurate and reliable verification, the ROI is needed to be detected for different thermal images of vein patterns share the same region. Figure 5a shows the ROI gained by the ROI extracting algorithm proposed in [8], where the second and

fourth finger webs are selected as the datum points to define a square ROI. The resolutions of the captured palm vein images are 640 × 480 while the size of the square ROI is approximately 128 × 128 with 256 gray levels. In our experiment, the 128 × 128 regions are resized to 64 × 64 pixels in the training and testing procedure, since the 64 × 64 resolution has been verified to be optimal for high-security biometric systems [11].

2.2 Image enhancement

In order to decrease costs, the applied CCD in our experiment is a cheap one, which leads to the poor quality of pictures. As a result, the contrast of the palm vein images is so awful that it is difficult to distinguish between palm veins and backgrounds visibly. Figure 2 shows the histogram statistics of the ROI where all the gray values gather up from 117 to 211 without obvious watershed between palm veins and backgrounds.

At first, the histogram equalization (HE) is employed here to enhance the contrast. However, experiments show that some gray values with less possession of pixels are gathered in HE, which results in blurry palm veins. Therefore, considering the drawbacks of HE, an improved version of HE, namely CLAHE is applied to maintain the image details and enhance the contrast between vein patterns and the backgrounds. The CLAHE is carried out by the way just like what is described in [15]:

Step1: Divide the image into a series of sub-regions
Step2: Clip the histograms of sub-regions based on clipping limits
Step3: Equalize the histograms of sub-regions
Step4: Interpolate every single pixel to get a new gray value

Figure 3 exhibits the enhancement results by HE and CLAHE. It is shown that the HE intensifies the contrast while blurs the details of the image. By comparison,
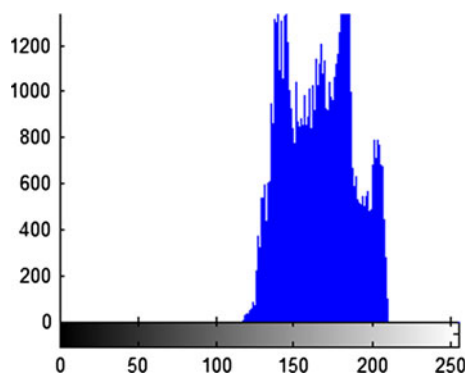
CLAHE can strike the balance between the contrast and the details effectively.

Then, there is a problem that palm veins and prints are both obviously visible in the image we have got. Therefore, to facilitate correct identification and matching, they are obliged to be processed in a way with palm veins remained and prints suppressed. In this section, a 2D Gaussian low-pass filter $H(\mu, \gamma) = e^{-D^2(\mu,\gamma)/2\sigma^2}$ with standard deviation $\sigma = 0.8$ is used to remove the palm prints effectively. As shown in Fig. 4, after the low-pass filtering, the vein patterns become smoother on their edges while the palm prints disappear as high-frequency signals. On the contrary, after the high-pass filter, while the contrast between vein patterns and background is enhanced, the palm veins are also highlighted.

2.3 Image segmentation

After the enhancement, palm veins and backgrounds contain less noise such as palm prints and high-frequency noise and are more easily distinguished. As the ultimate goal is to extract the vein pattern, it is needed to separate the veins from the backgrounds. The gray-level intensity values of both veins and backgrounds vary from one region to another in the image. And parts of them share the same location in the gray histogram instead of bimodal distribution. A single global thresholding is not enough for the image segmentation, while local thresholdings lead to shadows and manmade borders. Therefore, a dynamic thresholding [16] is necessary here to guarantee the accuracy and completeness of segmentation. Every pixel in the image is assigned a threshold on the analysis of its $n \times n$ neighborhoods. The image is binarized in a way as follows:

$$I'(x, y) = \begin{cases} 0, & i(x, y) < \text{th} \\ 255, & \text{otherwise} \end{cases} \quad (1)$$

where th is the mean value of its surrounding neighborhoods. And Fig. 5d shows the segmentation result using dynamic thresholding. The vein patterns are visibly separated from the background but with some noise remained to be removed.

Then, morphological opening and closing operations [17] are employed to remove isolated noise inside and outside the vein patterns. Here, the noise appears as the black elements in the background and the white elements embedded in the vein patterns. Noise elimination can be achieved by morphological filter consisted of opening operation followed by closing operation. The structural element of template we adopt for morphological opening and closing is a circular with radius of 3 pixels. The background noise is completely eliminated in the erosion process of opening operation for the reason that the physical dimensions of noises in background are mostly smaller

Fig. 2 Histogram of the ROI

Fig. 3 Enhancement results using two methods. *Left*: histogram equalization; *Right*: contrast limited adaptive histogram equalization
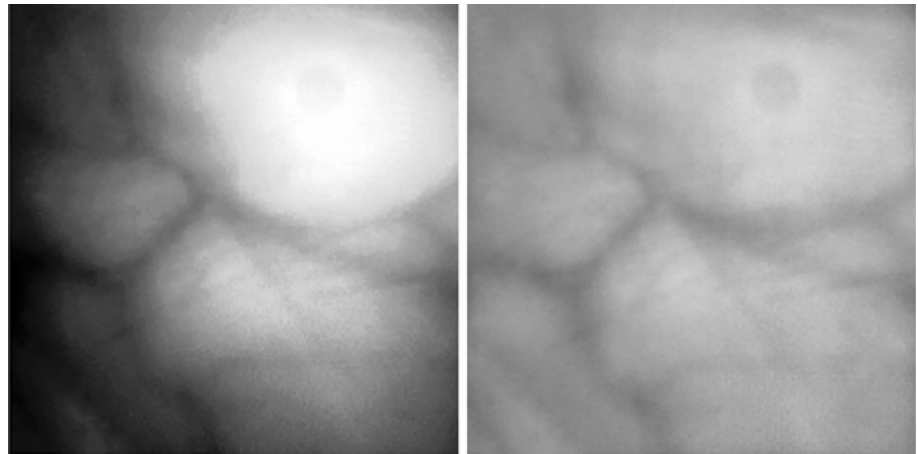

Fig. 4 Filtering results using two methods. *Left*: after high-pass filter; *Right*: after low-pass filter
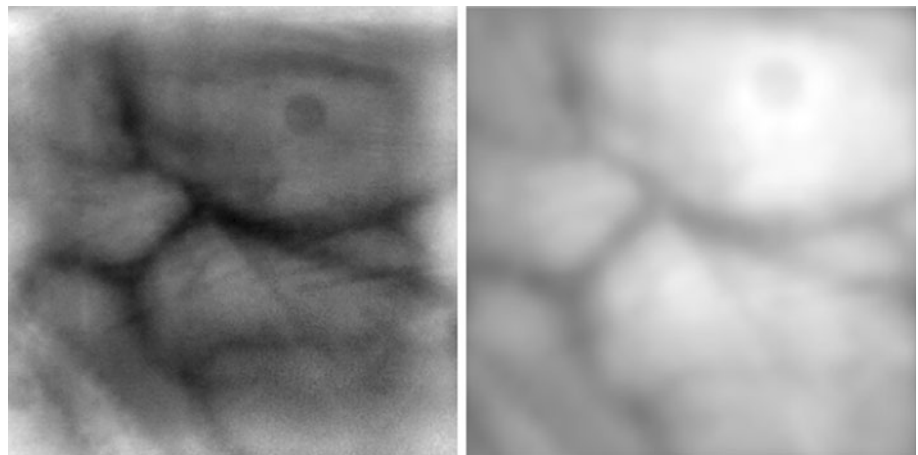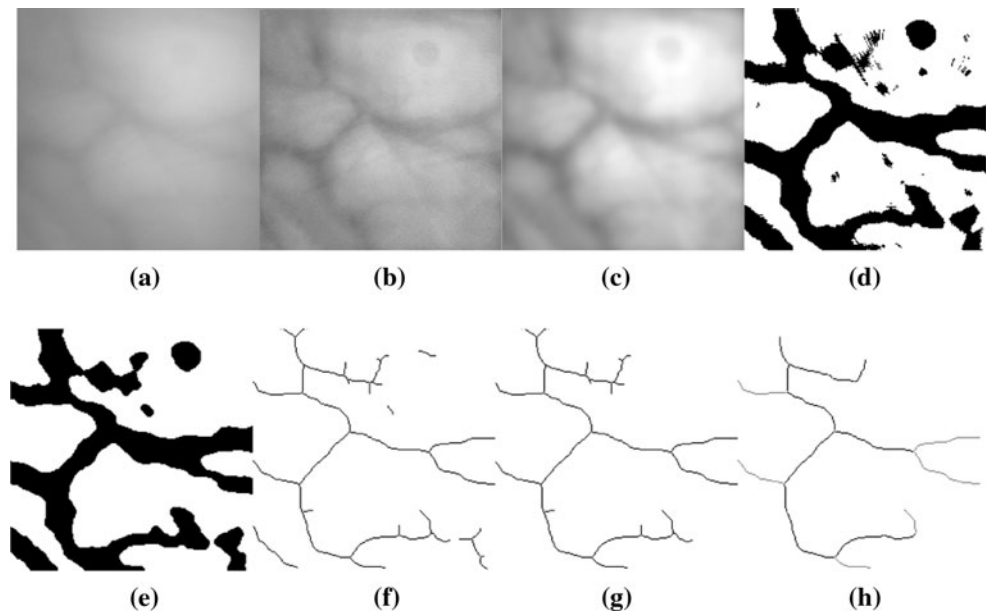

Fig. 5 Results of every procedure in palm vein identification (**a** region of interest, **b** CLAHE, **c** low-pass filter, **d** dynamic thresholding, **e** morphological opening and thinning closing operation, **f** template skeletonization, **g** isolated lines pruning, **h** short branches pruning)

(a)   (b)   (c)   (d)

(e)   (f)   (g)   (h)

than that of the structural element. The dimensions of noise embedded in the vein patterns are enlarged because those noises are dealt with as the internal border of vein patterns.

However, the noise in the vein patterns is reduced or even totally eliminated in the dilation process. As showed in Fig. 5e, after opening and closing operation, the noises are

Table 1 Different skeletonization templates

Direction	B	Direction	B
North	$\begin{pmatrix} 1 & 1 & 1 \\ 0 & 7 & 0 \\ -0.5 & -1 & -0.5 \end{pmatrix}$	Northwest	$\begin{pmatrix} 1 & 1 & 0 \\ 1 & 7 & -1 \\ 0 & -1 & 0 \end{pmatrix}$
Northeast	$\begin{pmatrix} 0 & 1 & 1 \\ -1 & 7 & 1 \\ 0 & -1 & 0 \end{pmatrix}$	West	$\begin{pmatrix} 1 & 0 & -0.5 \\ 1 & 7 & -1 \\ 1 & 0 & -0.5 \end{pmatrix}$
South	$\begin{pmatrix} -0.5 & -1 & -0.5 \\ 0 & 7 & 0 \\ 1 & 1 & 1 \end{pmatrix}$	Southwest	$\begin{pmatrix} 0 & -1 & 0 \\ 1 & 7 & -1 \\ 1 & 1 & 0 \end{pmatrix}$
Southeast	$\begin{pmatrix} 0 & -1 & 0 \\ -1 & 7 & 1 \\ 0 & 1 & 1 \end{pmatrix}$	East	$\begin{pmatrix} -0.5 & 0 & 1 \\ -1 & 7 & 1 \\ -0.5 & 0 & 1 \end{pmatrix}$

considerably diminished while some tolerable intermittent ones still exist.

2.4 Image skeletonization

As a matter of fact, image skeletonization is a processing method of thinning to acquire an image of vein patterns with a strictly single pixel width. Vein patterns are thinned in a way that the current pixel surroundings are divested step by step in eight directions until one single pixel left. And template operations shown in Table 1 are carried out in eight directions for skeletonization [18].

Some isolated pixels result from the above procedure. They can be removed using the template below.

$$A = 0, \quad B = \begin{pmatrix} 1 & 1 & 1 \\ 1 & 8 & 1 \\ 1 & 1 & 1 \end{pmatrix}, \quad i = -1 \tag{2}$$

Figure 5f shows that the palm vein image has been perfectly thinned until the width of contour occupies only single pixel. However, there are still some isolated lines and short branches in the image. So, we propose a pruning algorithm to remove them. The isolated line removal algorithm is described as follows:

Step1: Pick up all the possible end points including pseudo-end points

Step2: Climb along the streakline from current point. If another end point instead of the intersection point is touched firstly, the streakline is an isolated line and will be removed

Step3: Repeat step1 and step2 until reach the contour

The short branch pruning algorithm is stated below:

Step1: Pick up all the possible end points including pseudo-end points

Step2: Climb along the streakline from current point until intersection point is touched. If the branch

length is under the threshold T, the branch is thought as a short branch and removed, otherwise reserved

Step3: Repeat step1 and step2 until reach the contour

The pruning results are shown in Fig. 5g, h. It can be seen that after the pruning process, the skeletons of the vein pattern are successfully extracted and the shape of the vein pattern is well preserved.

2.5 Feature extraction and matching

Inspired by the feature extraction of palm prints [19], we take Gabor wavelet transform-based method to describe the texture of palm vein patterns for the sake of translation and rotation invariance. Gabor wavelet transform has multi-orientation properties and is optimal for measuring local spatial frequencies. Besides, it can yield distortion tolerance space for pattern recognition tasks [20]. Therefore, Gabor wavelet decomposition is suitable to extract feature eigenvectors for palm vein patterns.

The Gabor wavelet transform can be obtained as follows by using the expanding and rotation of mother function, giving $g(x,y)$ as the mother wavelet [21].

$$g_{mn}(x, y) = a^{-m}g(x', y'), a > 1, m, n \in \text{int} \tag{3}$$

where

$$g(x, y) = \frac{1}{2\pi\sigma_x\sigma_y}\exp\left(\frac{-1}{2}\left(\frac{x^2}{\sigma_x^2} + \frac{y^2}{\sigma_y^2}\right)\right)\exp(2\pi jWx) \tag{4}$$

$$x' = \alpha^{-m}(x\cos\theta + y\sin\theta) \tag{5}$$

$$y' = a^{-m}(-x\sin\theta + y\cos\theta) \tag{6}$$

where $\theta = n\pi/k$, k is the number of directions and a^{-m} is scale factor.

We use the wavelet basis above to structure a Gabor filter. It is worth noting that the skeleton image instead of the grayscale image is acted as the input image because the former has much less noises and can represent palm vein patterns more accurately. Therefore, the skeleton image $I(x, y)$ obtained in the last step is convoluted with a Gabor filter $g_{mn}(x, y)$ using the m th scale and the n th direction. Then, $m \times n$ different Gabor wavelet transformations of the image $I(x, y)$ are made through the following formula:

$$W_{mn}(x, y) = \sum_{i=1}^{M}\sum_{j=1}^{N}I(x, y)g_{mn}(x - i, y - j) \tag{7}$$

where $m = 0, 1, 2, 3$; $n = 0, 1, 2, 3, 4, 5$.

The mean μ_{mn} and standard deviation σ_{mn} of all transformed coefficients are obtained from Eqs. (8, 9), respectively.

$$u_{mn} = \frac{1}{M \times N} \sum_{i=1}^{M} \sum_{j=1}^{N} |W_{mn}(i,j)| \tag{8}$$

$$\sigma_{mn} = \sqrt{\frac{1}{M \times N} \sum_{i=1}^{M} \sum_{j=1}^{N} (W_{mn}(i,j) - u_{mn})^2} \tag{9}$$

Then, a 48 dimension eigenvector T is created by two basic elements μ_{mn} and σ_{mn}. It is described as following:

$$Y = [T_0, T_1, \cdots T_i, \cdots T_{46}, T_{47}] \tag{10}$$

Where $T_{2k} = \mu_{mn}$, $T_{2k+1} = \sigma_{mn}$.

As described in [22], the element order should be based on the dominant direction and a simple circular shift on the feature eigenvector is employed to solve the rotation variance problem. Here, the total energy for each orientation is calculated. And the orientation with the highest total energy is called the dominant orientation. The feature elements in dominant orientation are moved and selected as the first element in the feature vector. Then, the other elements are circularly shifted.

Finally, we adopt correlation coefficient [19] to make the classification decision.

$$R_{s_1 s_2} = \frac{l_{s_1 s_2} \times l_{s_1 s_2}}{l_{s_1 s_1} \times l_{s_2 s_2}} \tag{11}$$

where

$$l_{s_1 s_2} = \sum_{i=1}^{n} (s_1 - \bar{s}_1)(s_2 - \bar{s}_2) \tag{12}$$

$$l_{s_1 s_1} = \sum_{i=1}^{n} (s_1 - \bar{s}_1)^2 \tag{13}$$

$$l_{s_2 s_2} = \sum_{i=1}^{n} (s_2 - \bar{s}_2)^2 \tag{14}$$

If $R_{s_1 s_2} > T_h$, then the two palm vein patterns belong to the same person. If $R_{s_1 s_2} \leq T_l$, they are not the same and rejection is decided.

3 Experimental results and discussion

In our experiments, a total number of 683 palm vein images were collected from 101 persons over a period of 3 months to evaluate our proposed method. Among them, the testing database and the training database are mutual exclusive, with 505 palm vein images used as training samples and the rest 178 images for testing. Also, it should be noted that the 505 training images are made up of palm vein images from the 101 persons with 5 images for each subject. The size of each ROI image was 64×64 resolution with 256 gray levels. To evaluate the effectiveness of

the proposed method, the experiments were implemented in two modes: identification and verification. In the identification mode, the correct recognition rate (CRR) was adopted to evaluate the effectiveness of our method. In the verification mode, the receiver operating characteristic (ROC) curve was used to depict the relationship between the false rejection rate (FRR) and the false acceptance rate (FAR).

This section uses three experiments to demonstrate the performance of the proposed method for palm vein recognition. The first experiment shows the validity of every step of preprocessing to enhance the structure of palm vein patterns and suppress unwanted noises and disturbances effectively. The second one analyzes the relationship between the recognition accuracy and different palm vein pattern representations: skeleton image or grayscale one. Finally, the third one gives the comparisons and discussions between our method and the three existing methods. The following subsections will present the experiments and results in detail.

3.1 Performance evaluation of the proposed method

Owing to the shape uniqueness of vein patterns, we proposed a new method to recognize vein patterns, which contains ROI extraction; image enhancement including CLAHE and 2-D Gaussian low-pass filtering; image segmentation with dynamic thresholding and morphological opening and closing operation; image skeletonization using template thinning followed by isolated lines and short branches elimination and vein pattern extraction and matching based on Gabor wavelet features.

Figure 5 is an example that we give every step to show the validity of our measures. In this figure, a is the original image, b is an enhancement of a with CLAHE and c is a filtered image of b by using a 2D Gaussian low-pass filter. It can be seen that the contrast in b between palm veins and background has been enhanced obviously while the details of the image are retained, and the vein patterns in c become smoother with their edges while the palm prints disappear as the high-frequency signals. Then, we make use of dynamic thresholding to segment c and accomplish the image shown in d in spite of brightness fluctuations in c. And e is d with noises removed and edges smoothed by morphological opening and closing operator. Template operation is employed to thin e and get a preferable result shown in f. g and h demonstrate the vein patterns after isolate lines and short branches have been eliminated, respectively.

In the second test, we evaluate the performance using Gabor wavelet features of palm vein patterns extracted from two different kinds of images: skeleton and grayscale. A total of 178 comparisons are performed on the basis of
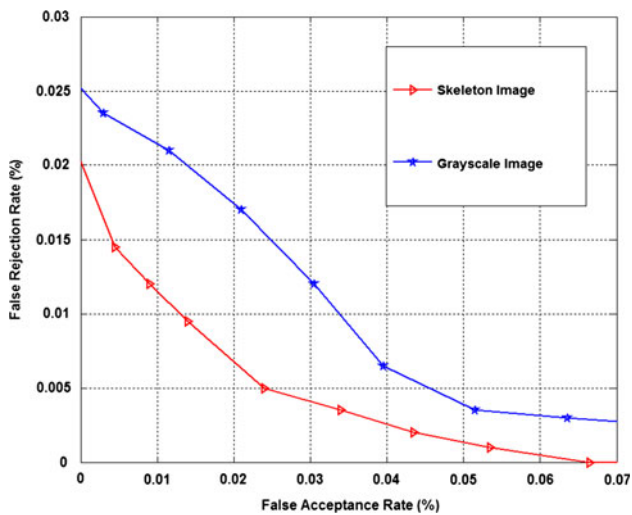
Fig. 6 ROC curves at two kinds of images: skeleton image (*red*) and grayscale image (*blue*)

all the testing images. The feature vector of each kind of testing image is matched against their stored template, respectively. The ROC curves, which plots the FAR against FRR, are chosen to analyze the performance of the experimental results. Figure 6 illustrates the FAR and FRR distributions of the two kinds of images. It displays that the whole curve of the skeleton image is below that of the grayscale one. That is, the Gabor wavelet features from skeleton images are more suitable than those from grayscale ones in our database. This may be generated from two facts. Firstly, the palm vein patterns are much more obvious in the skeleton image than in the grayscale image. Secondly, the grayscale image may suffer from the remaining noises such as palm prints or light sports.

3.2 Comparison and discussion

The experimental results in Sect. 3.1 demonstrate that the proposed method is effective for palm vein pattern recognition in our database. And the methods proposed in [9, 11, 12] are well known for palm vein recognition. Hence, we compare our method with these three methods in order to further prove our methods' effectiveness. For the sake of fairness, together with our proposed approach, all these methods are tested by using our own database with 178 testing samples from 101 persons. It also should be noted that our experimental results of each algorithm are consistent with their published results, which to some extent shows our correct implementations of other methods. Table 2 and Fig. 7 show the comparisons of the experimental results in detail.

The four different methods are all quite effective as their successful rates (CRR) shown in Table 2 exceed 95 %. As

Table 2 Performance comparison of four different methods on our database

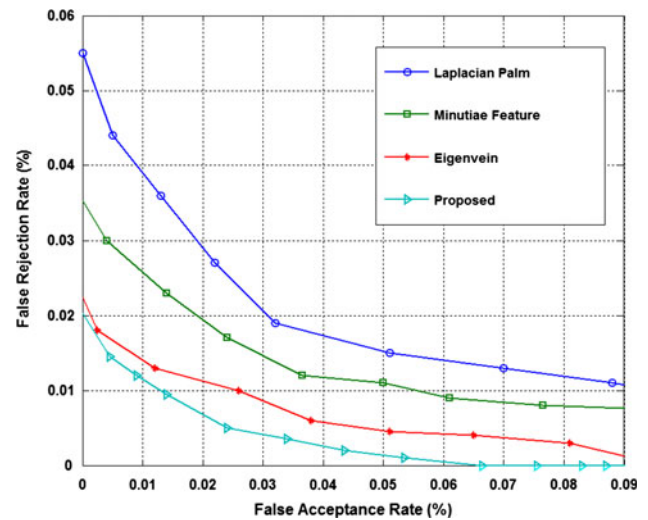| Methods	Right match	Wrong match	Rejection	Successful rate (%)
Minutiae feature	174	2	2	97.75
Laplacianpalm	172	4	2	96.63
Eigenvein	175	2	1	98.31
Proposed	176	1	1	98.88

Fig. 7 ROC curves of four methods

for the proposed method, there are 178 vein patterns for testing in our database and we achieved 176 successful recognitions and two failures. One of the failures is an instance of incorrectly identifying an unauthorized person, and the other is an occurrence of failing to identify an authorized person. The ROC curves of the four methods on our own database are displayed in Fig. 7. They demonstrate that our method is slightly better than the other three popular methods. The accuracy of the geometric-based method [9] may be affected by information loss because the features of palm vein pattern are only represented by the geometric information of minutiae points such as branching points and ending points. In the method based on Laplacianpalm [12], palm veins are fused with palm prints for the representation of palm features. However, palm prints are not stable enough for they may change as a result of wear, injury, aging and different health conditions. While the eigenvein method [11] preserves the global structure of the palm vein image, the local textured information is lost. In addition, since the eigenveins obtained by 2DPCA are sensitive to rotation variations which are quite common and inevitable in the stage of data acquisition, the accuracy may be influenced. From Table 2 and Fig. 7, we

can see that the proposed method obtain slightly better performance than other methods. It is the result of the following three reasons. Firstly, on the preprocessing stage, a series of well-known techniques has been applied to enhance the contrast between palm veins and backgrounds and eliminate negative influences produced by unwanted noises and disturbances such as palm prints, light spots and so on. Secondly, the Gabor wavelet features can effectively analyze variations in the intensity, which can reflect most of the random shape information of the palm vein and thus achieve a slightly higher performance. Meanwhile, due to the translation and rotation invariance of Gabor wavelet features, our method can accurately align the rotation and shift variations introduced in data acquisition to some extent.

The proposed method is implemented in Visual C++. It runs on the computing environment of 2.2 GHz PC with 2 GB RAM. The average computation time costs for image preprocessing, feature extraction and matching are 76, 248 ms and 15 μs, respectively. The total computation time is about 324 ms, which can meet the real-time requirements.

4 Conclusions and future work

The framework of an automated thermal palm vein pattern recognition system was developed in this paper. Its operation can be divided into five image processing phases: image acquisition, enhancement, segmentation, skeletonization, feature extraction and matching. The proposed method achieves good performance proved by the experiments using 683 palm vein images. It can overcome the problem of rotation and shift essentially owing to the Gabor wavelet's advantages. In particular, this method has many advantages over the other methods. Firstly, our CCD is a very cheap one which considerably cuts the cost and thus is touched with preferable completion. Secondly, compared with palm-dorsa vein patterns for verification, the palm vein patterns are more difficult to be revealed due to thicker skins with palm prints as noises. Finally, the method is relatively simple and practical.

Our future work will focus on two aspects. First, the global and local features of the vein patterns are supposed to be effectively exploited by combining Gabor wavelet features with the space pyramid technique. Also, the speed of the system could be improved when a fast Gabor transform is available or the transform is precomputed.

References

1. Yangqiang Z, Dongmei S, Zhengding Q (2012) Hand-based single sample biometrics recognition. Neural Comput Appl 21(8):1835–1844
2. Soni M, Gupta S, Rao MS, Gupta P (2010) A new vein pattern-based verification system. Int J Comput Sci Inform Secur 8(1):58–63
3. Doublet J, Lepetit O, Revenu M (2007) Contactless palmprint authentication using circular gabor filter and approximated string matching. In: Proceedings of international conference on signal and image processing (SIP), Honolulu, pp 511–516
4. Wang L, Leedham G (2005) A thermal hand vein pattern verification system. In: Proceedings of international conference on pattern recognition and image analysis, LNCS 3687, pp 58–65
5. Chen H-F, Lu G-M, Wang R (2009) A new palm vein matching method based on ICP algorithm. In: Proceedings of international conference on interaction sciences: information technology, culture and human, Seoul, Korea, pp 1207–1211
6. Li X-Y, Guo S-X, Gao F-L, Li Y (2007) Vein pattern recognitions by moment invariants. In: Proceedings of international conference of bioinfomatics and biomedical engineering, Wuhan, China, pp 612–615
7. Yang JC, Xie SJ, Yoon S, Park DS, Fang ZJ, Yang SY (2013) Fingerprint matching based on extreme learning machine. Neural Comput Appl 22(3–4):435–445
8. Fan KC, Lin CL, Lee WL (2004) Biometric verification using thermal images of palm-dorsa vein patterns. IEEE Trans Circuits Syst Video Technol 14(2):199–213
9. Wang LY, Leedham G, Cho DS (2008) Minutiae feature analysis for infrared hand vein pattern biometrics. Pattern Recogn 41(3):450–453
10. Zhang YB, Li Q, Yan J, Bhattacharya P (2007) Palm vein extraction and matching for personal authentication. In: Proceeding of international conference on advances in visual information systems, LNCS 4781, pp 154–164
11. Hsu CB, Hao SS, Lee JC (2011) Personal authentication through dorsal hand vein patterns. Opt Eng 50(8):087201.1–087201.10
12. Wang JG, Yau WY, Suwandy A, Sung E (2008) Person recognition by fusing palmprint and palm vein images based on "Laplacianpalm" representation. Pattern Recogn 41(5):1514–1527
13. Lee JC (2012) A novel biometric system based on palm vein image. Pattern Recogn Lett 33(12):1520–1528
14. Zhang B, Qiao Y (2010) Face recognition based on gradient gabor feature and efficient kernel fisher analysis. Neural Comput Appl 19(4):617–623
15. Liu X, Liu JB (2008) Mammary image enhancement based on contrast limited adaptive histogram equalization. Comput Eng Appl 44(10):173–175
16. Wang KJ, Ding YH, Zhuang DY, Wang DZ (2005) Threshold segmentation for hand vein image. Tech Autom Appl 24(8):19–22
17. Gonzalez RC, Woods RE Digital image processing. Published by arrangement with the original publisher, Pearson Education, Inc., publishing as Prentice Hall, ISBN: 0201180758
18. Suleyman M, Yu FQ, Lambert S (2006) Vein feature extraction using DT-CNNs. Int workshop on cellular neural networks and their applications 1–6
19. Li Y, Wu GF, Dai GL, Li JJ (2010) A new algorithm to extract contour feature points of palmprint. Microelectron Comput 27(5):90–94
20. Shen LL, Bai L (2006) A review of Gabor wavelets for face recognition. Pattern Anal Appl 9(2–3):273–292
21. Li JB, Pan JS, Lu ZM (2009) Face recognition using Gabor-based complete kernel fisher discriminant analysis with fractional power polynomial models. Neural Comput Appl 18(6):613–621
22. Arivazhagan S, Ganesan L, Priyal SP (2006) Texture classification using Gabor wavelets based rotation invariant features. Pattern Recogn Lett 27(16):1976–1982